Acta Crystallographica Section B
Structural Science
ISSN 0108-7681

Nine *N*-aryl-2-chloronicotinamides: supramolecular structures in one, two and three dimensions

Silvia Cuffini,[a] Christopher Glidewell,[b]* John N. Low,[c] Aline G. de Oliveira,[d] Marcus V. N. de Souza,[d] Thatyana R. A. Vasconcelos,[d] Solange M. S. V. Wardell[d] and James L. Wardell[e]

[a]Agência Córdoba Ciência-Unidad Ceprocor, Córdoba, Argentina, [b]School of Chemistry, University of St Andrews, St Andrews, Fife KY16 9ST, Scotland, [c]Department of Chemistry, University of Aberdeen, Meston Walk, Old Aberdeen AB24 3UE, Scotland, [d]Fundação Oswaldo Cruz, Far Manguinhos, Rua Sizenando Nabuco, 100 Manguinhos, 21041-250 Rio de Janeiro-RJ, Brazil, and [e]Instituto de Química, Departamento de Química Inorgânica, Universidade Federal do Rio de Janeiro, CP 68563, 21945-970 Rio de Janeiro-RJ, Brazil

Correspondence e-mail: cg@st-andrews.ac.uk

Received 28 January 2006
Accepted 27 April 2006

Structures are reported here for eight further substituted *N*-aryl-2-chloronicotinamides, 2-$ClC_5H_3NCONHC_6H_4X$-4′. When X = H, compound (I) ($C_{12}H_9ClN_2O$), the molecules are linked into sheets by N—H···N, C—H···π(pyridyl) and C—H···π(arene) hydrogen bonds. For X = CH_3, compound (II) ($C_{13}H_{11}ClN_2O$, triclinic $P\bar{1}$ with Z' = 2), the molecules are linked into sheets by N—H···O, C—H···O and C—H···π(arene) hydrogen bonds. Compound (III), where X = F, crystallizes as a monohydrate ($C_{12}H_8ClFN_2O\cdot H_2O$) and sheets are formed by N—H···O, O—H···O and O—H···N hydrogen bonds and aromatic $\pi\cdots\pi$ stacking interactions. Crystals of compound (IV), where X = Cl ($C_{12}H_8Cl_2N_2O$, monoclinic $P2_1$ with Z' = 4) exhibit inversion twinning: the molecules are linked by N—H···O hydrogen bonds into four independent chains, linked in pairs by C—H···π(arene) hydrogen bonds. When X = Br, compound (V) ($C_{12}H_8BrClN_2O$), the molecules are linked into sheets by N—H···O and C—H···N hydrogen bonds, while in compound (VI), where X = I ($C_{12}H_8ClIN_2O$), the molecules are linked into a three-dimensional framework by N—H···O and C—H···π(arene) hydrogen bonds and an iodo···N(pyridyl) interaction. For X = CH_3O, compound (VII) ($C_{13}H_{11}ClN_2O_2$), the molecules are linked into chains by a single N—H···O hydrogen bond. Compound (VIII) ($C_{13}H_8ClN_3O$, triclinic $P\bar{1}$ with Z' = 2), where X = CN, forms a complex three-dimensional framework by N—H···N, C—H···N and C—H···O hydrogen bonds and two independent aromatic $\pi\cdots\pi$ stacking interactions.

1. Introduction

Nicotinic acid (pyridine-3-carboxylic acid) and nicotinamide (niacinamide, pyridine-3-carboxamide) are two of the principal members of the B-vitamin complex. Niacin, nicotinamide and nicotinic acid have identical vitamin activities, but they have very different pharmacological activities. Nicotinamide, *via* its major metabolite nicotinamide adenine dinucleotide, is involved in a wide range of biological processes including the production of energy, the synthesis of fatty acids, cholesterol and steroids, signal transduction, and the maintenance of the integrity of the genome. Nicotinic acid in pharmacological doses is used as an antihyperlipidemic agent: it also causes vasodilation of cutaneous blood vessels. Nicotinamide has been investigated as an agent for the prevention or delay of the onset of type 1 diabetes mellitus. It also has anti-oxidant, anti-inflammatory and anti-carcinogenic activities, and has putative activity against osteoarthritis and granuloma annulare. We have made a study of the properties and activities of substituted derivatives, 2-chloro-*N*-(4-*X*-phenyl)nicotina-

mides, and here we report the structures and supramolecular arrangements of nine examples having X = H (I), Me (II), F (III), Cl (IV), Br (V), I (VI), OMe (VII) and CN (VIII), and including the recently reported analogue with $X = NO_2$, (IX) (de Souza *et al.*, 2005).

Here we report the molecular and supramolecular structures of eight closely related *N*-aryl-2-chloronicotinamides, 2-$ClC_5H_3NCONHC_6H_4X$-4′, whose crystallization characteristics prove to be all different, even within the halogen-substituted subset, (III)–(VI), and whose supramolecular structures all prove to be different, with no two utilizing the same combination of direction-specific intermolecular interactions.

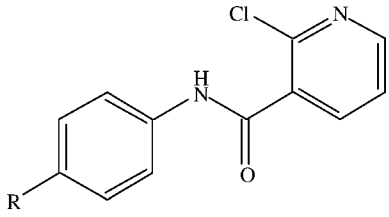

(I) R = H
(II) R = CH_3
(III) R = F
(IV) R = Cl
(V) R = Br
(VI) R = I
(VII) R = OCH_3
(VIII) R = CN
(IX) R = NO_2

2. Experimental

2.1. Synthesis

Samples of (I)–(VIII) were prepared by reaction of equimolar quantities of 2-chloronicotinoyl chloride and the appropriate substituted aniline in tetrahydrofuran solution at ambient temperature in the presence of a catalytic quantity of triethylamine. After stirring for 8 h, the reaction mixtures were neutralized with saturated aqueous sodium hydrogencarbonate solution and the resulting aqueous mixtures were extracted with ethyl acetate (2×30 cm^3). For each preparation, the organic extracts were combined, dried over anhydrous sodium sulfate, and then concentrated under reduced pressure. Chromatography on silica, using hexane:ethyl acetate gradients (up to 50% ethyl acetate), then yielded the pure products, with yields in the range 80–90%. Crystals of (I), (II) and (IV)–(VIII) suitable for single-crystal X-ray diffraction were grown from solution in ethanol, and crystals of (III) were grown from an aqueous solution: m.p.s: (I) 395–397 K, (II) 432–433 K, (III) 366–367 K, (IV) 421–422 K, (V) 399–400 K, (VI) 448–450 K, (VII) 383–384 K and (VIII) 445–446 K.

2.2. Data collection, structure solution and refinement

Details of cell data, data collection and structure solution and refinement are summarized in Table 1 (Bruker, 2004; Cernik *et al.*, 1997; Ferguson, 1999; McArdle, 2003; Otwinowski & Minor, 1997; Sheldrick, 1997*a*,*b*, 2003; Hooft, 1999). The space groups for (I), (IV), (V), VI) and (VII) were all assigned uniquely from the systematic absences: crystals of (II), (III) and (VIII) are triclinic, and for each the space group $P\bar{1}$ was selected, and confirmed by the successful structure analysis. The structures were all solved by direct methods using *SHELXS*97 (Sheldrick, 1997*a*) and refined on F^2 with all data using *SHELXL*97 (Sheldrick, 1997*b*). A weighting scheme based upon $P = [F_o^2 + 2F_c^2]/3$ was employed in order to reduce statistical bias (Wilson, 1976). All H atoms were located from difference maps and all were included in the refinements as riding atoms, with distances C—H 0.95 and N—H 0.88 Å, and with $U_{iso}(H) = 1.2U_{eq}(C,N)$. For (V) and (VII), the correct enantiomorph was selected using the Flack parameter (Flack, 1983): the final values were 0.031 (7) and −0.05 (7), respectively. For (IV), where the crystals were all of very poor quality, the Flack parameter 0.54 (11) indicated inversion twinning.

Supramolecular analyses were made and the diagrams were prepared with the aid of *PLATON* (Spek, 2003). Figs. 1–30 show the independent components of (I)–(VIII) and aspects of their supramolecular structures. Selected torsional angles are given in Table 2 and details of the hydrogen bonding are in Table 3.[1]

3. Results and discussion

3.1. Crystallization characteristics

Compounds (II) and (VIII) both crystallize with Z' = 2, while (IV) has Z'= 4; similarly, the 4-nitrophenyl derivative (IX) crystallizes with Z' = 2 (de Souza *et al.*, 2005). Of the compounds (I)–(VIII) reported here, the 4-fluorophenyl derivative is unique in crystallizing as a monohydrate, although the 2-nitrophenyl analogue reported recently (de Souza *et al.*, 2005) also crystallizes as a stoichiometric monohydrate.

3.2. Molecular conformations

In each of compounds (I)–(VIII), as well as in (IX) (de Souza *et al.*, 2005), the central C—C—N—C spacer unit is nearly planar, as shown by the torsional angles for this unit which are all close to 180°, ranging between 170.0 (3) and −173.4 (2)° (Table 2). However, the aryl ring is often markedly twisted out of this plane, particularly in (II), (IV), (V), (VI) and (VII), while the chloropyridyl is always twisted well away from the plane of the central spacer, being nearly orthogonal to this plane in (II), (VI), (VIII) and (IX). An alternative way to consider the overall conformations is by

[1] Supplementary data for this paper are available from the IUCr electronic archives (Reference: BM5033). Services for accessing these data are described at the back of the journal.

Table 1
Experimental details.

	(I)	(II)	(III)	(IV)
Crystal data				
Chemical formula	$C_{12}H_9ClN_2O$	$C_{13}H_{11}ClN_2O$	$C_{12}H_8ClFN_2O\cdot H_2O$	$C_{12}H_8Cl_2N_2O$
M_r	232.66	246.69	268.67	267.10
Cell setting, space group	Orthorhombic, *Pccn*	Triclinic, $P\bar{1}$	Triclinic, $P\bar{1}$	Monoclinic, $P2_1$
Temperature (K)	120 (2)	120 (2)	120 (2)	120 (2)
a, *b*, *c* (Å)	13.2296 (6), 21.0744 (10), 7.6898 (16)	9.6824 (6), 11.3082 (7), 11.5139 (7)	6.8033 (4), 8.1303 (3), 11.5356 (6)	5.0855 (8), 28.982 (8), 15.607 (4)
α, β, γ (°)	90, 90, 90	77.453 (2), 73.445 (2), 87.978 (2)	84.032 (3), 84.297 (2), 69.569 (3)	90, 90.37 (2), 90
V (Å^3)	2144.0 (5)	1179.07 (13)	593.32 (5)	2300.2 (9)
Z	8	4	2	8
D_x (Mg m^{-3})	1.442	1.390	1.504	1.543
Radiation type	Mo $K\alpha$	Synchrotron, λ = 0.67510 Å	Mo $K\alpha$	Mo $K\alpha$
No. of reflections for cell parameters	2446	6881	2720	9787
θ range (°)	3.1–27.5	2.1–28.8	3.3–27.8	3.0–27.5
μ (mm^{-1})	0.33	0.31	0.33	0.55
Crystal form, colour	Needle, colourless	Needle, colourless	Plate, colourless	Plate, colourless
Crystal size (mm)	0.24 × 0.09 × 0.02	0.10 × 0.02 × 0.02	0.18 × 0.16 × 0.03	0.28 × 0.07 × 0.03
Data collection				
Diffractometer	Bruker–Nonius 95 mm CCD camera on κ goniostat	Bruker SMART APEX2 CCD diffractometer	Bruker–Nonius 95 mm CCD camera on κ goniostat	Bruker–Nonius 95 mm CCD camera on κ goniostat
Data collection method	φ and ω scans	Fine-slice ω scans	φ and ω scans	φ and ω scans
Absorption correction	Multi-scan	Multi-scan	Multi-scan	Multi-scan
T_{min}	0.943	0.970	0.933	0.862
T_{max}	0.993	0.994	0.990	0.984
No. of measured, independent and observed reflections	17 837, 2446, 1724	12 982, 6881, 5217	12 303, 2720, 1943	24 726, 9787, 6370
Criterion for observed reflections	$I > 2\sigma(I)$	$I > 2\sigma(I)$	$I > 2\sigma(I)$	$I > 2\sigma(I)$
R_{int}	0.104	0.022	0.052	0.053
θ_{max} (°)	27.5	28.8	27.8	27.5
Range of *h*, *k*, *l*	$-16 \Rightarrow h \Rightarrow 17$ $-27 \Rightarrow k \Rightarrow 27$ $-9 \Rightarrow l \Rightarrow 9$	$-13 \Rightarrow h \Rightarrow 13$ $-16 \Rightarrow k \Rightarrow 16$ $-16 \Rightarrow l \Rightarrow 16$	$-8 \Rightarrow h \Rightarrow 8$ $-9 \Rightarrow k \Rightarrow 10$ $-14 \Rightarrow l \Rightarrow 14$	$-6 \Rightarrow h \Rightarrow 6$ $-37 \Rightarrow k \Rightarrow 37$ $-20 \Rightarrow l \Rightarrow 20$
Refinement				
Refinement on	F^2	F^2	F^2	F^2
$R[F^2 > 2\sigma(F^2)]$, $wR(F^2)$, S	0.059, 0.129, 1.07	0.044, 0.124, 1.02	0.044, 0.113, 1.05	0.069, 0.169, 1.04
No. of reflections	2446	6881	2720	9787
No. of parameters	145	309	163	254
H-atom treatment	Constrained to parent site	Constrained to parent site	Constrained to parent site	Constrained to parent site
Weighting scheme	$w = 1/[\sigma^2(F_o^2) + (0.0479P)^2 + 1.6007P]$, where $P = (F_o^2 + 2F_c^2)/3$	$w = 1/[\sigma^2(F_o^2) + (0.0648P)^2 + 0.3225P]$, where $P = (F_o^2 + 2F_c^2)/3$	$w = 1/[\sigma^2(F_o^2) + (0.0536P)^2 + 0.1705P]$, where $P = (F_o^2 + 2F_c^2)/3$	$w = 1/[\sigma^2(F_o^2) + (0.0454P)^2 + 5.774P]$, where $P = (F_o^2 + 2F_c^2)/3$
$(\Delta/\sigma)_{max}$	0.001	0.001	<0.0001	0.001
$\Delta\rho_{max}$, $\Delta\rho_{min}$ (e Å^{-3})	0.28, −0.28	0.43, −0.30	0.26, −0.29	0.79, −0.54
Absolute structure	–	–	–	Flack (1983), 4396 Friedel pairs
Flack parameter	–	–	–	0.54 (11)

	(V)	(VI)	(VII)	(VIII)
Crystal data				
Chemical formula	$C_{12}H_8BrClN_2O$	$C_{12}H_8ClIN_2O$	$C_{13}H_{11}ClN_2O_2$	$C_{13}H_8ClN_3O$
M_r	311.56	358.55	262.69	257.67
Cell setting, space group	Orthorhombic, $P2_12_12_1$	Orthorhombic, *Pbca*	Orthorhombic, $P2_12_12_1$	Triclinic, $P\bar{1}$
Temperature (K)	120 (2)	120 (2)	120 (2)	120 (2)
a, *b*, *c* (Å)	4.8810 (2), 13.3448 (2), 18.3974 (3)	10.6597 (2), 25.9833 (3), 9.2044 (6)	4.8536 (2), 11.8437 (4), 21.0612 (7)	7.2885 (3), 7.7607 (3), 20.8849 (9)
α, β, γ (°)	90, 90, 90	90, 90, 90	90, 90, 90	96.456 (2), 92.913 (2), 91.810 (2)
V (Å^3)	1198.33 (6)	2549.38 (18)	1210.69 (6)	1171.49 (8)
Z	4	8	4	4
D_x (Mg m^{-3})	1.727	1.868	1.441	1.461
Radiation type	Mo $K\alpha$	Mo $K\alpha$	Mo $K\alpha$	Mo $K\alpha$

Table 1 (continued)

	(V)	(VI)	(VII)	(VIII)
No. of reflections for cell parameters	2736	2909	2661	5365
θ range (°)	3.0–27.5	3.0–27.5	3.6–27.5	2.9–27.6
μ (mm^{-1})	3.64	2.71	0.31	0.32
Crystal form, colour	Block, colourless	Plate, colourless	Block, colourless	Block, colourless
Crystal size (mm)	0.16 × 0.16 × 0.16	0.33 × 0.18 × 0.07	0.34 × 0.22 × 0.12	0.40 × 0.10 × 0.10
Data collection				
Diffractometer	Bruker–Nonius 95 mm CCD camera on κ goniostat	Bruker–Nonius 95 mm CCD camera on κ goniostat	Bruker–Nonius 95 mm CCD camera on κ goniostat	Bruker–Nonius 95 mm CCD camera on κ goniostat
Data collection method	φ and ω scans	φ and ω scans	φ and ω scans	φ and ω scans
Absorption correction	Multi-scan	Multi-scan	Multi-scan	Multi-scan
T_{min}	0.558	0.469	0.921	0.899
T_{max}	0.558	0.833	0.964	0.969
No. of measured, independent and observed reflections	36 201, 2736, 2597	19 649, 2909, 2314	7884, 2661, 2184	21 639, 5365, 3760
Criterion for observed reflections	$I > 2\sigma(I)$	$I > 2\sigma(I)$	$I > 2\sigma(I)$	$I > 2\sigma(I)$
R_{int}	0.047	0.038	0.040	0.060
θ_{max} (°)	27.5	27.5	27.5	27.6
Range of h, k, l	$-6 \Rightarrow h \Rightarrow 6$ $-17 \Rightarrow k \Rightarrow 17$ $-23 \Rightarrow l \Rightarrow 23$	$-13 \Rightarrow h \Rightarrow 13$ $-32 \Rightarrow k \Rightarrow 33$ $-11 \Rightarrow l \Rightarrow 11$	$-5 \Rightarrow h \Rightarrow 6$ $-15 \Rightarrow k \Rightarrow 11$ $-21 \Rightarrow l \Rightarrow 27$	$-9 \Rightarrow h \Rightarrow 9$ $-10 \Rightarrow k \Rightarrow 10$ $-27 \Rightarrow l \Rightarrow 26$
Refinement				
Refinement on	F^2	F^2	F^2	F^2
$R[F^2 > 2\sigma(F^2)]$, $wR(F^2)$, S	0.023, 0.060, 1.07	0.023, 0.056, 1.04	0.042, 0.104, 1.04	0.059, 0.171, 1.06
No. of reflections	2736	2909	2661	5365
No. of parameters	154	154	164	325
H-atom treatment	Constrained to parent site	Constrained to parent site	Constrained to parent site	Constrained to parent site
Weighting scheme	$w = 1/[\sigma^2(F_o^2) + (0.0339P)^2 + 0.2964P]$, where $P = (F_o^2 + 2F_c^2)/3$	$w = 1/[\sigma^2(F_o^2) + (0.026P)^2 + 0.5926P]$, where $P = (F_o^2 + 2F_c^2)/3$	$w = 1/[\sigma^2(F_o^2) + (0.0579P)^2]$, where $P = (F_o^2 + 2F_c^2)/3$	$w = 1/[\sigma^2(F_o^2) + (0.0844P)^2 + 1.0407P]$, where $P = (F_o^2 + 2F_c^2)/3$
$(\Delta/\sigma)_{max}$	0.001	0.005	<0.0001	<0.0001
$\Delta\rho_{max}$, $\Delta\rho_{min}$ (e Å^{-3})	0.43, −0.52	0.39, −0.78	0.24, −0.35	0.74, −0.35
Absolute structure	Flack (1983), 1098 Friedel pairs	–	Flack (1983), 1013 Friedel pairs	–
Flack parameter	0.031 (7)	–	−0.05 (7)	–

means of the dihedral angle denoted Δ between the two rings of each molecule, also shown in Table 2. It is striking to note the relationships between the conformations of the four independent molecules in (IV), shown particularly clearly by the dihedral angles Δ: molecules 1 and 2, containing N21 and N41 respectively, are close to being enantiomorphs, as are molecules 3 and 4 containing N61 and N81. However, the relationships between molecules 1 and 3, and between molecules 2 and 4 is that of diastereoisomers. The wide range of the dihedral angles Δ in (I)–(IX), varying from 10.2 (2)° in (VII) to 89.4 (2)° in molecule 2 of (VIII), indicates that the intramolecular barriers to rotation about the C—C bonds connecting the rings to the central spacer unit are rather readily overcome by the intermolecular forces, in particular by the direction-specific hydrogen bonds. In this way the observed conformations are an indirect reflection of the action of the hydrogen bonds, just as the detailed supramolecular aggregation patterns are a direct reflection of the action of the hydrogen bonds. The bond lengths and angles present no unusual features.

3.3. Supramolecular structures

3.3.1. Compound (I). In the unsubstituted parent compound, (I) (Fig. 1), the molecules are linked into sheets by a combination of N—H···N, C—H···π(pyridyl) and C—H···π(arene) hydrogen bonds, but N—H···O hydrogen bonds are absent (Table 3). The formation of the sheets is most conveniently analysed and described in terms of the chains formed by the N—H···N and C—H···π(pyridyl) hydrogen bonds, and the linkage of the chains by the C—H···π(arene) hydrogen bonds.

The amidic N21 atom in the molecule at (x, y, z) acts as a hydrogen-bond donor to the pyridyl N11 atom in the molecule at $(\frac{1}{2} - x, y, -\frac{1}{2} + z)$, thus forming a $C(7)$ (Bernstein *et al.*, 1995) chain running parallel to the [001] direction and generated by the c glide plane at $x = 0.25$. This chain is reinforced by the —H···π(pyridyl) hydrogen bond, where the C16 atom in the molecule at (x, y, z) acts as a donor to the pyridyl ring in the molecule at $(\frac{1}{2} - x, y, \frac{1}{2} + z)$, thus forming a [001] chain of rings generated by the c glide plane at $y = 0.25$ (Fig. 2).

Table 2
Selected torsional and dihedral angles (°).

C13—C17—N21—C21	C12—C13—C17—N21	C17—N21—C21—C22	Δ†
(I)			
178.8 (2)	−56.2 (4)	−171.8 (2)	48.2 (2)
(II)			
175.30 (13)	−99.53 (16)	−141.82 (15)	59.8 (2)
175.77 (13)‡	−103.14 (16)†	166.05 (14)†	62.9 (2)
(III)			
171.39 (18)	130.5 (2)	174.60 (18)	62.6 (2)
(IV)			
175.0 (6)	135.5 (8)	149.0 (6)	78.2 (3)
−176.7 (6)‡	−137.9 (8)†	−148.6 (5)†	77.8 (3)
173.9 (6)‡	134.4 (8)†	−141.9 (6)†	12.4 (3)
−176.9 (6)‡	−138.0 (8)†	144.9 (5)†	11.5 (3)
(V)			
178.86 (17)	51.3 (3)	143.6 (2)	17.2 (2)
(VI)			
172.75 (19)	−77.3 (2)	−135.9 (2)	35.4 (2)
(VII)			
−179.41 (18)	−134.5 (2)	141.0 (2)	10.2 (2)
(VIII)			
170.3 (3)	−73.7 (4)	−163.6 (3)	60.9 (2)
−174.2 (3)‡	90.9 (3)†	177.8 (3)†	89.4 (3)
(IX)§			
173.29 (19)	78.1 (3)	−179.8 (2)	73.3 (2)
−173.4 (2)‡	−71.5 (3)†	173.6 (2)†	73.6 (3)

† Δ is the dihedral angle between the two rings in each independent molecule. ‡ In molecule 2 of (II), (IV), (VIII) and (IX) the relevant atom sequence is C32—C33—C37—N41—C41—C42; in molecules 3 and 4 of (IV) the relevant atom sequences are C52—C53—C57—N61—C61—C62 and C72—C73—C77—N81—C81—C82, respectively (see Figs. 5, 12 and 25). § Data from de Souza *et al.* (2005).

Four chains of this type pass though each unit cell, two each in the domains $0.25 < y < 0.75$ and $-0.25 < y < 0.25$, and within each domain, one chain is generated by the *c* glide plane at 0.25, and the other, antiparallel to the first, is generated by the *c* glide plane at $y = 0.75$. A simple centrosymmetric motif serves to link the antiparallel pairs of [001] chains in each domain to form sheets. The C15 atom in the molecule at (x, y, z), which is part of a chain generated by the glide plane at $x = 0.25$, acts as a hydrogen-bond donor to the phenyl ring in the molecule at $(1 - x, 1 - y, 1 - z)$, which is part of a chain generated by the glide plane at $x = 0.75$ (Fig. 3). Propagation of this interaction then links all the chains in a given domain of *y* into a (010) sheet (Fig. 4): two sheets, related to one another by the twofold rotation axes parallel to [001], pass through each unit cell, but there are no direction-specific interactions between adjacent sheets.

3.3.2. Compound (II). In the 4-methylphenyl derivative (II), where $Z' = 2$ (Fig. 5), the molecules are linked by two independent N—H···O hydrogen bonds (Table 3) into $C_2^2(8)$ chains (Fig. 6): it is convenient to refer to molecules containing atoms O1 and O3 as 1 and 2, respectively. Two antiparallel $C_2^2(8)$ chains pass through each unit cell and these chains are linked into a chain of edge-fused rings by a single, nearly linear C—H···O hydrogen bond, where the pyridyl C35 atom in molecule 2 at (x, y, z) acts as a hydrogen-bond donor to the O1 atom in molecule 1 at $(1 - x, 1 - y, 1 - z)$. Propagation by translation and inversion of these three hydrogen bonds, two of the N—H···O type and one of the C—H···O type, generates a chain of centrosymmetric, edge-fused rings along $(x, \frac{1}{2}, \frac{1}{2})$, with $R_4^2(16)$ rings centred at $(n, \frac{1}{2}, \frac{1}{2})$ (n = zero or integer) and $R_4^4(20)$ rings centred at $(n + \frac{1}{2}, \frac{1}{2}, \frac{1}{2})$ (n = zero or integer; Fig. 7).

There are two C—H···π(arene) hydrogen bonds in the structure of (II) (Table 3): one, having the C34 atom as the donor, lies within the [100] chain of rings, but the other, having C14 as the donor, links the [100] chains into sheets. The C14 atom in molecule 1 at (x, y, z) lies in the chain along $(x, \frac{1}{2}, \frac{1}{2})$: this atom acts as a donor to the phenyl ring C41–C46 in molecule 2 at $(1 - x, 2 - y, -z)$, which lies in the chain along $(x, \frac{3}{2}, -\frac{1}{2})$. Propagation by inversion of this C—H···π(arene) hydrogen bond then links [100] chains into a (011) sheet (Fig. 8). There are no direction-specific interactions between adjacent sheets.

3.3.3. Compound (III). The 4-fluorophenyl derivative crystallizes as a monohydrate, compound (III), and in the selected asymmetric unit (Fig. 9) the two components are linked by an N—H···O hydrogen bond: this utilization of the N—H donor site immediately precludes the formation of the characteristic amidic $C(4)$ chain. Instead the molecules are linked into chains of edge-fused rings by a combination of O—H···O and O—H···N hydrogen bonds (Table 3), and these chains are linked into sheets by a single aromatic $\pi\cdots\pi$ stacking interaction.

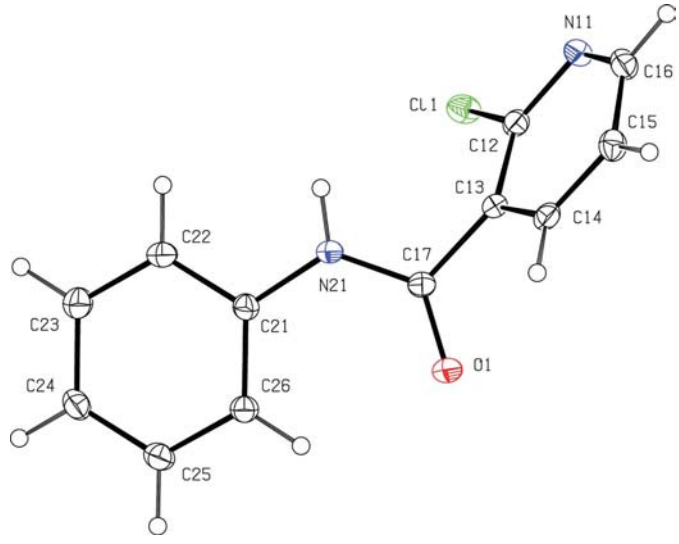

Figure 1
The molecule of (I) showing the atom-labelling scheme. Displacement ellipsoids are drawn at the 30% probability level.

The water atom O2 at (x, y, z) acts as a hydrogen-bond donor, *via* H2*B*, to the amidic atom O1 at $(-1+x, y, z)$, thus generating by translation a $C_2^2(6)$ chain running parallel to the [100] direction. An antiparallel pair of these $C_2^2(6)$ chains is linked by the N—H···O hydrogen bond: the O2 atom at (x, y, z) acts as a donor, *via* H2*A*, to the pyridyl N11 atom at $(1-x, 2-y, 1-z)$, thus generating a centrosymmetric $R_4^4(16)$ ring, centred at $(\frac{1}{2}, 1, \frac{1}{2})$. The combination of all the hydrogen bonds then generates, by translation and inversion, a chain of edge-fused $R_4^4(16)$ rings along $(x, 1, \frac{1}{2})$ (Fig. 10). There are two types of ring within this chain and both are centrosymmetric: those having amidic O atoms as two of the acceptor sites are centred at $(n, 1, \frac{1}{2})$ (n = zero or integer), and

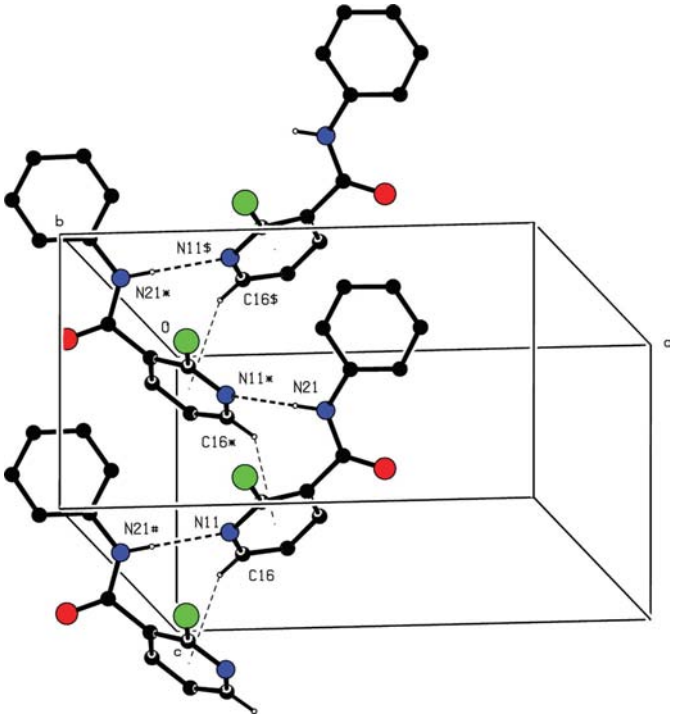

Figure 2
Part of the crystal structure of (I) showing the formation of a hydrogen-bonded chain of rings along [001]. For the sake of clarity, the H atoms not involved in the motifs shown have been omitted. The atoms marked with an asterisk (*), a hash (#) or a dollar sign ($) are at the symmetry positions $(\frac{1}{2}-x, y-\frac{1}{2}+z)$, $(\frac{1}{2}-x, y, \frac{1}{2}+z)$ and $(x, y, -1+z)$, respectively.

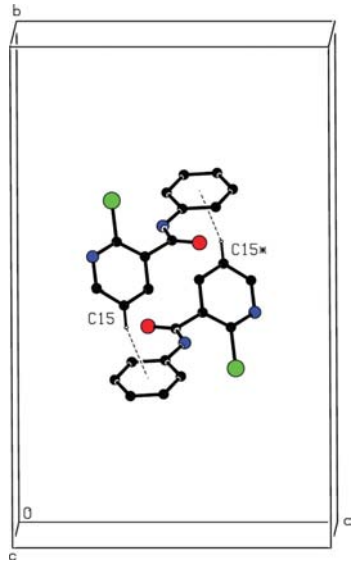

Figure 3
Part of the crystal structure of (I) showing the centrosymmetric ring built from C—H···π(arene) hydrogen bonds, which link the [001] chains into (010) sheets. For the sake of clarity, the H atoms not involved in the motif shown have been omitted. The atom marked with an asterisk (*) is at the symmetry position $(1-x, 1-y, 1-z)$.

Table 3
Hydrogen-bond parameters (Å, °).

D—H···A	H···A	D···A	D—H···A
(I)			
N21—H21···N11^{i}	2.25	3.101 (3)	164
C15—H15···Cg1^{ii}†	2.89	3.535 (3)	126
C16—H16···Cg2^{iii}‡	2.87	3.464 (3)	121
(II)			
N21—H21···O3	1.96	2.827 (2)	170
N41—H41···O1^{iv}	1.99	2.847 (2)	163
C35—H35···O1^{ii}	2.48	3.424 (2)	174
C14—H14···Cg3^{v}§	2.69	3.398 (2)	132
C34—H34···Cg2^{ii}‡	2.63	3.398 (2)	138
(III)			
N21—H21···O2	1.91	2.837 (2)	179
O2—H2*A*···N11^{vi}	1.97	2.887 (2)	161
O2—H2*B*···O1^{iv}	1.95	2.780 (2)	173
(IV)			
N21—H21···O1^{iv}	2.11	2.925 (8)	153
N41—H41···O3^{iv}	2.00	2.833 (8)	157
N61—H61···O5^{vii}	2.11	2.925 (8)	153
N81—H81···O7^{vii}	2.00	2.841 (8)	159
C26—H26···Cg5¶	2.76	3.444 (8)	130
C46—H46···Cg4††	2.75	3.448 (8)	131
C62—H62···Cg3^{vii}§	2.88	3.588 (8)	132
C82—H82···Cg2^{vii}‡	2.87	3.579 (8)	132
(V)			
N21—H21···O1^{iv}	2.03	2.825 (2)	169
C22—H22···N11^{viii}	2.56	3.405 (3)	148
(VI)			
N21—H21···O1^{ix}	2.01	2.853 (2)	160
C15—H15···Cg2^{x}‡	2.65	3.404 (2)	137
(VII)			
N21—H21···O1^{ii}	1.92	2.785 (2)	168
(VIII)			
N21—H21···N44	2.15	3.006 (4)	164
N41—H41···N24^{xi}	2.10	2.978 (4)	173
C14—H14···O11^{xii}	2.49	3.334 (4)	148
C15—H15···O11^{ii}	2.60	3.507 (4)	160
C25—H25···N11^{xiii}	2.52	3.348 (4)	146
C34—H34···O31^{xiv}	2.53	3.327 (4)	142
C35—H35···O31^{ii}	2.45	3.366 (4)	161
C45—H45···N31^{xiii}	2.53	3.300 (4)	138

Symmetry codes: (i) $\frac{1}{2}-x, y, -\frac{1}{2}+z$; (ii) $1-x, 1-y, 1-z$; (iii) $\frac{1}{2}-x, y, \frac{1}{2}+z$; (iv) $-1+x, y, z$; (v) $1-x, 2-y, -z$; (vi) $1-x, 2-y, 1-z$; (vii) $1+x, y, z$; (viii) $-x, \frac{1}{2}+y, \frac{1}{2}-z$; (ix) $x, \frac{1}{2}-y, \frac{1}{2}+z$; (x) $-\frac{1}{2}+x, \frac{1}{2}-y, 1-z$; (xi) $-2+x, 1+y, z$; (xii) $1-x, -y, 1-z$; (xiii) $1+x, -1+y, z$; (xiv) $-1-x, 1-y, -z$. † Cg1 is the centroid of ring N11, C12–C16. ‡ Cg2 is the centroid of ring C21–C26. § Cg3 is the centroid of ring C41–C46. ¶ Cg5 is the centroid of ring C81–C86. †† Cg4 is the centroid of ring C61–C66.

those having water O atoms as two of the acceptor sites are centred at $(n+\frac{1}{2}, 1, \frac{1}{2})$ (n = zero or integer).

The pyridyl rings in the amide molecules at (x, y, z) and $(1-x, 1-y, 2-z)$ are strictly parallel with an interplanar spacing of 3.352 (2) Å; the ring-centroid separation is 3.618 (2) Å, corresponding to a nearly ideal ring offset of 1.362 (2) Å. These two amide molecules form parts of the chains of fused rings along $(x, 1, \frac{1}{2})$ and $(x, 0, \frac{3}{2})$, so that propagation by inversion of this stacking interaction forms a $[01\bar{1}]$ chain (Fig. 11), which links the chains of rings into a (011) sheet.

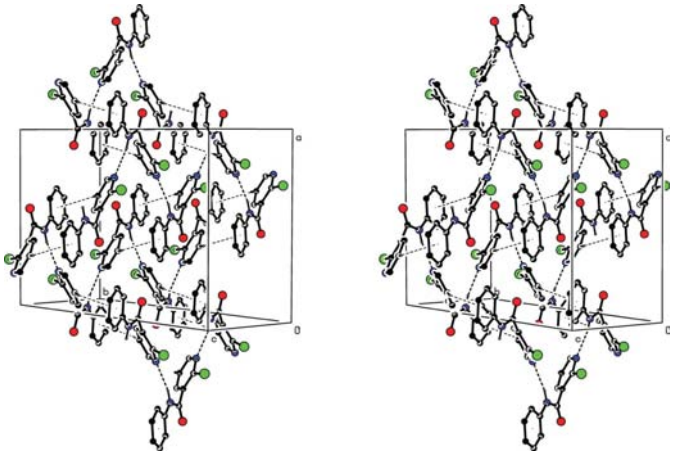

Figure 4
Stereoview of part of the crystal structure of (I), showing a hydrogen-bonded (010) sheet. For the sake of clarity, the H atoms not involved in the motifs shown have been omitted.

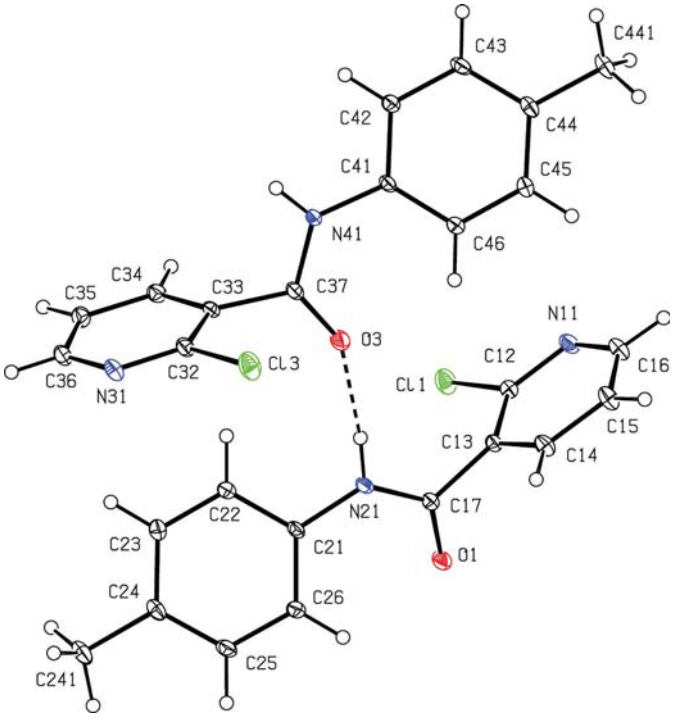

Figure 5
The two independent molecules of (II) showing the atom-labelling scheme and the N—H···O hydrogen bond within the asymmetric unit. Displacement ellipsoids are drawn at the 30% probability level.

3.3.4. Compound (IV). We comment here only briefly on the supramolecular aggregation of the 4-chlorophenyl compound (IV). This compound crystallizes in the non-centrosymmetric space group $P2_1$ with $Z' = 4$ (Fig. 12), but the crystal quality was extremely poor, with extensive twinning. Nonetheless, the main features of the structure are clear enough: each of the four independent molecules forms a $C(4)$ chain by translation along [100], built from N—H···O hydrogen bonds (Fig. 13), and these chains are linked in pairs by the C—H···π(arene) hydrogen bonds (Table 3).

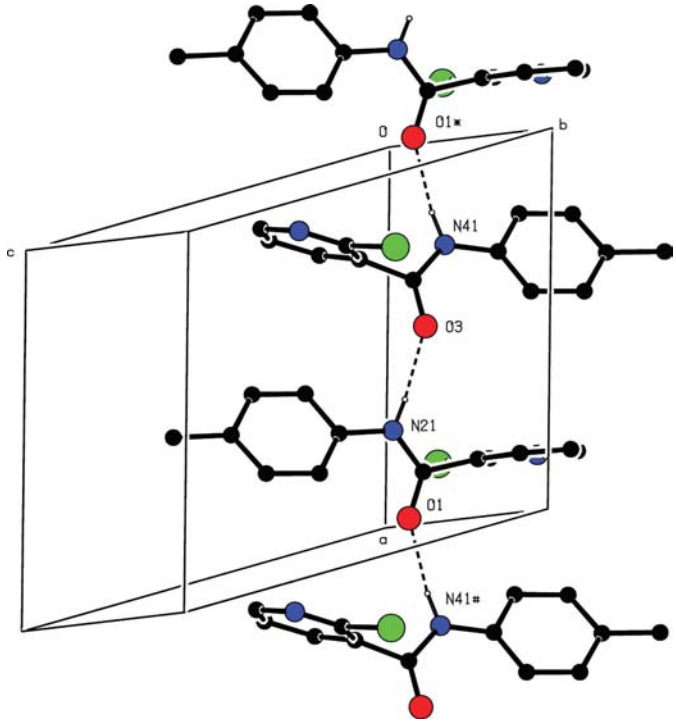

Figure 6
Part of the crystal structure of (II), showing the formation of a $C_2^2(8)$ chain along [100]. For the sake of clarity, the H atoms bonded to C atoms have been omitted. The atoms marked with an asterisk (*) or a hash (#) are at the symmetry positions $(-1+x, y, z)$ and $(1+x, y, z)$, respectively.

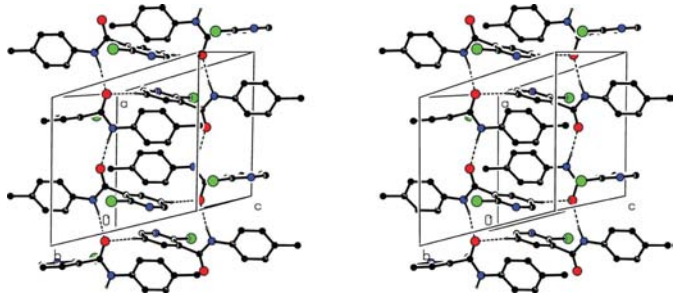

Figure 7
Stereoview of part of the crystal structure of (II) showing the formation of a chain of edge fused $R_4^2(16)$ and $R_4^4(20)$ rings along [100]. For the sake of clarity, the H atoms not involved in the motifs shown have been omitted.

3.3.5. Compound (V). In the 4-bromophenyl compound (V) (Fig. 14), the molecules are linked into isolated sheets by a combination of one N—H···O and one C—H···N hydrogen bond (Table 3). The amidic N21 atom in the molecule at (x, y, z) acts as a hydrogen-bond donor to the amidic O1 in the molecule at $(-1 + x, y, z)$, so generating by translation a $C(4)$ chain running parallel to the [100] direction (Fig. 15). Four chains of this type pass through each unit cell, two in each of the domains $0 < z < 0.5$ and $0.5 < z < 1.0$, and within each of these domains the chains are linked into sheets by a single C—H···N hydrogen bond. The aryl C22 atom in the molecule at (x, y, z) acts as a hydrogen-bond donor to the pyridyl N11 atom in the molecule at $(-x, \frac{1}{2} + y, \frac{1}{2} - z)$, so forming a $C(8)$ chain running parallel to the [010] direction, and generated by the 2_1 screw axis along $(0, y, \frac{1}{4})$ (Fig. 16). The combination of the [100] and [010] chains then generates a (001) sheet in the form of a (4,4) net built from a single type of $R_4^4(22)$ ring (Fig.

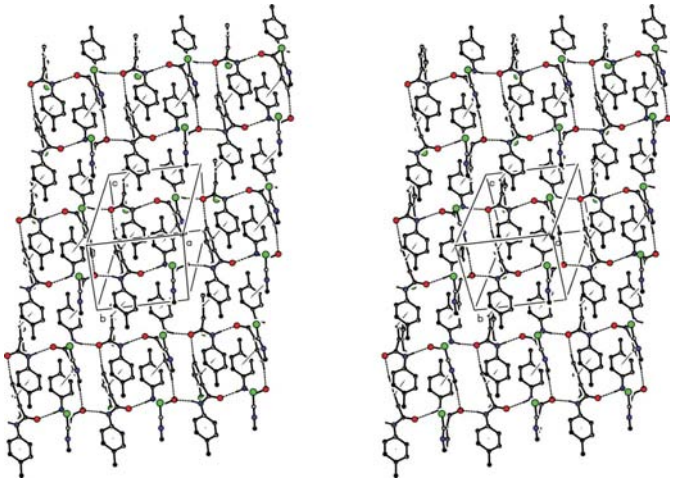

Figure 8
Stereoview of part of the crystal structure of (II) showing the linking, by means of a single C—H···π(arene) hydrogen bond, of the [100] chains of rings into a (011) sheet. For the sake of clarity, the H atoms not involved in the motifs shown have been omitted.

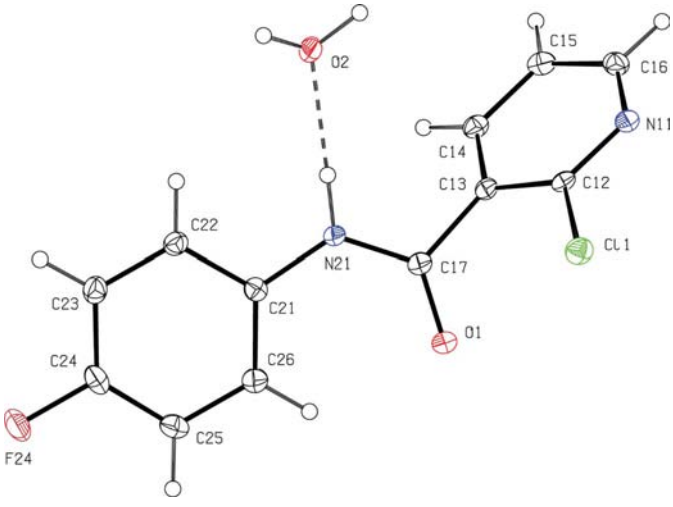

Figure 9
The molecular components of (III) showing the atom-labelling scheme. Displacement ellipsoids are drawn at the 30% probability level.

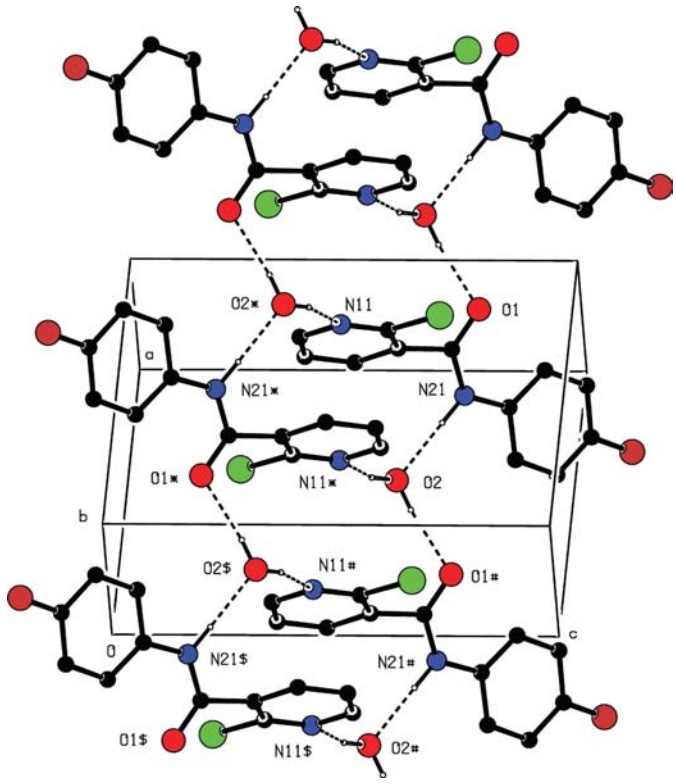

Figure 10
Part of the crystal structure of (III) showing the formation of a hydrogen-bonded chain of edge-fused rings along [100]. For the sake of clarity, the H atoms bonded to C atoms have been omitted. The atoms marked with an asterisk (*), a hash (#) or a dollar sign ($) are at the symmetry positions $(1 - x, 2 - y, 1 - z)$, $(-1 + x, y, z)$ and $(-x, 2 - y, 1 - z)$, respectively.

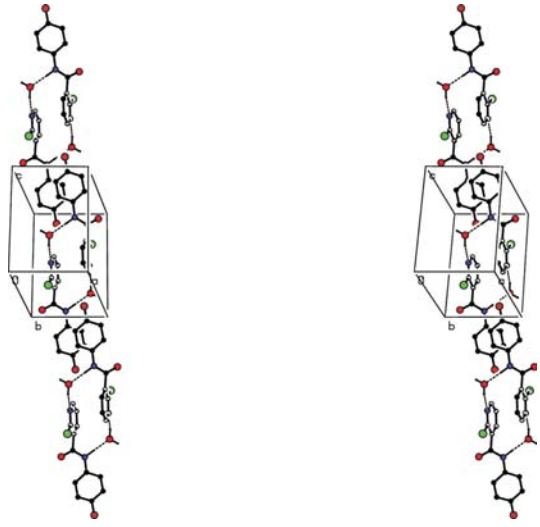

Figure 11
Stereoview of part of the crystal structure of (III) showing the centrosymmetric π-stacking interaction which links the [100] chains into (011) sheets. For the sake of clarity, the H atoms bonded to C atoms have been omitted.

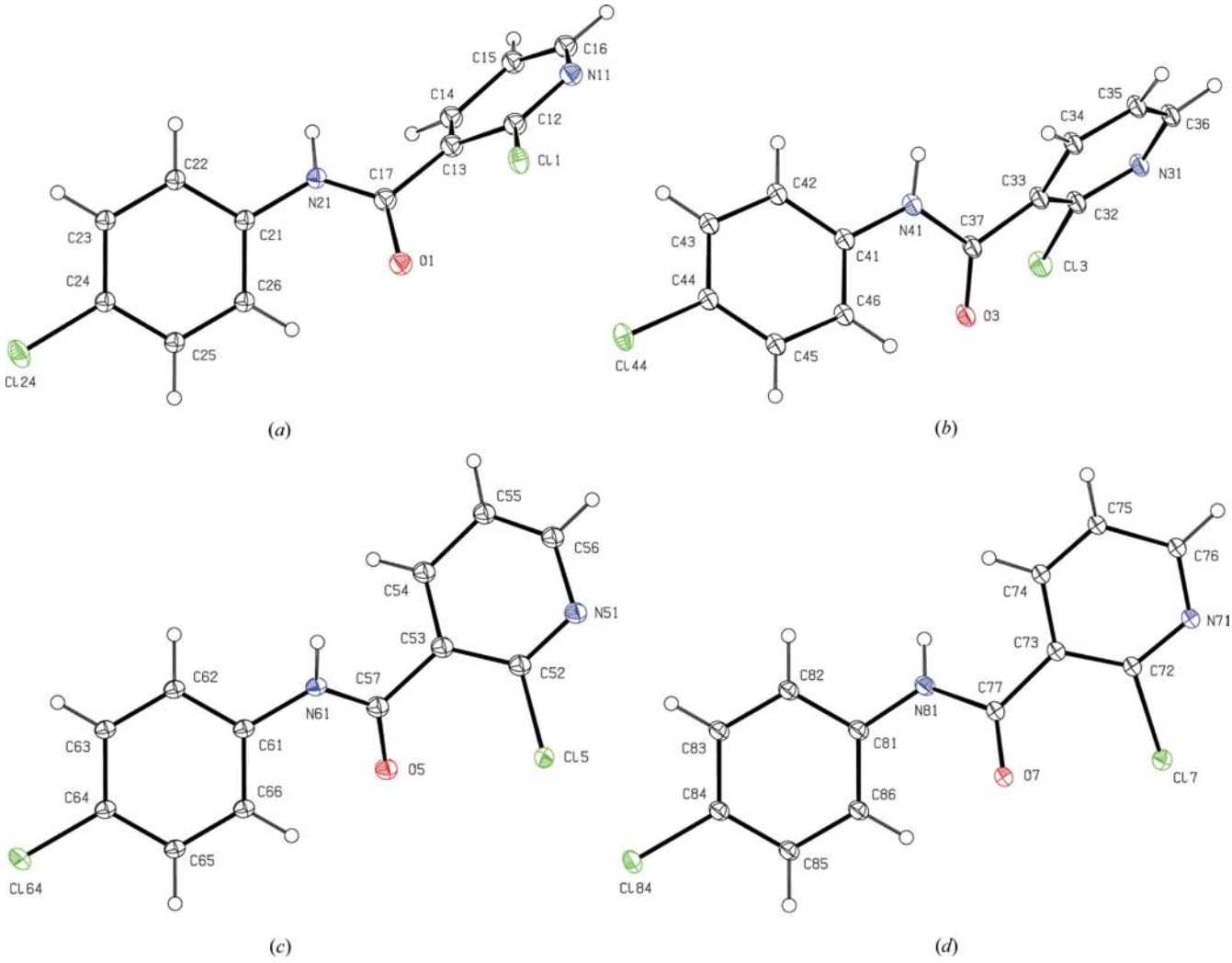

Figure 12
The four independent molecules of (IV) showing the atom-labelling scheme. Displacement ellipsoids are drawn at the 30% probability level. The atom labelling for the other three molecules and the conformational differences between the molecules are defined in Table 2.

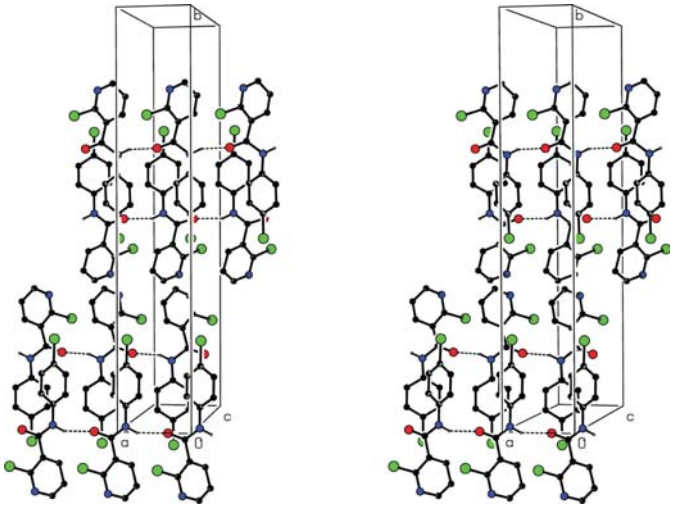

Figure 13
Stereoview of part of the crystal structure of (IV) showing the formation of four independent $C(4)$ chains along [100]. For the sake of clarity, the H atoms bonded to C atoms have been omitted.

17). Two sheets of this type pass through each unit cell, generated by screw axes at $y = 0.25$ and $y = 0.75$, respectively, but there are no direction-specific interactions between adjacent sheets: in particular, aromatic $\pi\cdots\pi$ stacking interactions and C—H$\cdots\pi$(arene) hydrogen bonds are absent.

3.3.6. Compound (VI). The molecules of the 4-iodophenyl compound (VI) (Fig. 18) are linked into sheets by a combination of one N—H$\cdots$O hydrogen bond and one C—H$\cdots\pi$(arene) hydrogen bond (Table 3) and these sheets are themselves linked by a single iodo$\cdots$N(pyridyl) interaction. The N21 atom in the molecule at (x, y, z) acts as a hydrogen-bond donor to the O1 atom in the molecule at $(x, \frac{1}{2} - y, \frac{1}{2} + z)$, so forming a $C(4)$ chain running parallel to the [001] direction, and generated by the c-glide plane at $y = 0.25$ (Fig. 19). In addition, the pyridyl C15 atom in the molecule at (x, y, z) acts as a hydrogen-bond donor to the aryl ring C21—C26 in the molecule at $(-\frac{1}{2} + x, \frac{1}{2} - y, 1 - z)$, so forming a chain running parallel to the [100] direction and generated by the 2_1 screw axis along $(x, \frac{1}{4}, \frac{1}{2})$ (Fig. 20). The combination of these two

hydrogen-bonded motifs then generates a (010) sheet (Fig. 21): two sheets of this type pass through each unit cell, in the domains $-0.02 < y < 0.52$ and $0.48 < y < 1.02$. The sole direction-specific interaction between adjacent sheets is an iodo···N(pyridyl) interaction, somewhat analogous electronically to an iodo···nitro interaction: the I24 atom in the molecule at (x, y, z) forms a short contact with the pyridyl N11 atom in the molecule at $(\frac{3}{2} - x, \frac{1}{2} + y, z)$, with dimensions I···N^{i} 3.116 (2) Å, C—I···N^{i} 167.5 (2)° [symmetry code (i) $\frac{3}{2} - x, \frac{1}{2} + y, z$]. This interaction thus forms a $C(10)$ chain (Starbuck *et al.*, 1999) running parallel to the [010] direction and generated by a *b*-glide plane at $y = 0.75$ (Fig. 22): in this manner all the (010) sheets are linked into a continuous three-dimensional array.

3.3.7. Compound (VII). The supramolecular aggregation of the 4-methoxyphenyl derivative, compound (VII) (Fig. 23), is exceptionally simple. A single N—H···O hydrogen bond (Table 3) links the molecules into $C(4)$ chains generated by translation (Fig. 24). Four chain of this type pass through each unit cell, but there are no direction-specific interactions between adjacent chains: in particular, C—H···π(arene)

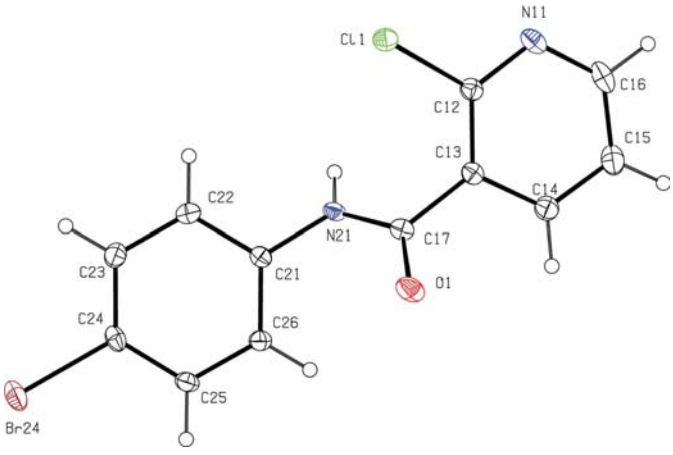

Figure 14
The molecule of (V) showing the atom-labelling scheme. Displacement ellipsoids are drawn at the 30% probability level.

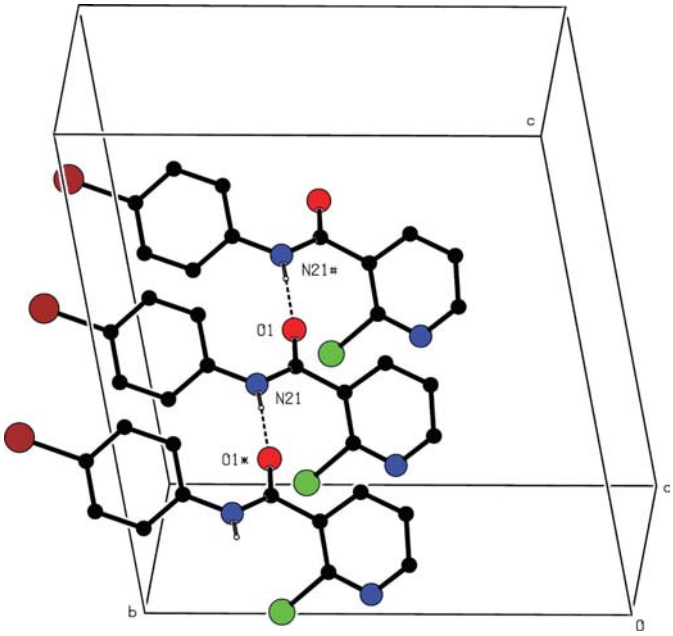

Figure 15
Part of the crystal structure of (V) showing the formation of a hydrogen-bonded $C(4)$ chain along [100]. For the sake of clarity, the H atoms bonded to C atoms have been omitted. The atoms marked with an asterisk (*) or a hash (#) are at the symmetry positions $(-1 + x, y, z)$ and $(1 + x, y, z)$, respectively.

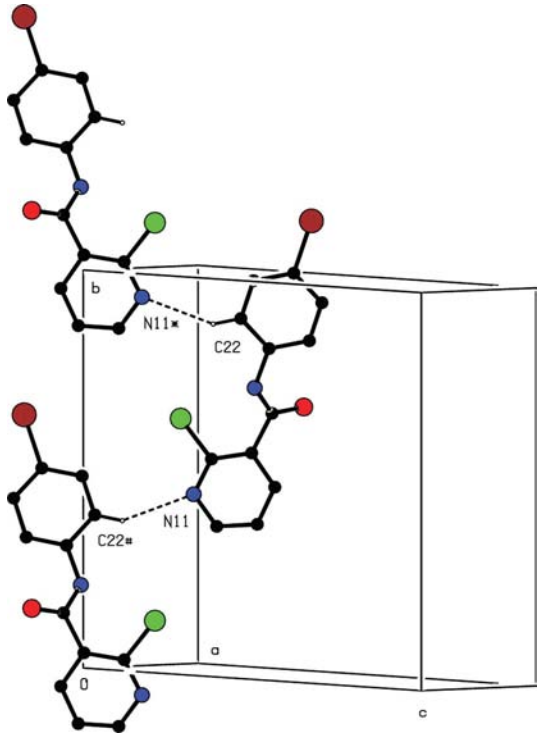

Figure 16
Part of the crystal structure of (V) showing the formation of a hydrogen-bonded $C(8)$ chain along [010]. For the sake of clarity, the H atoms not involved in the motif shown have been omitted. The atoms marked with an asterisk (*) or a hash (#) are at the symmetry positions $(-x, \frac{1}{2} + y, \frac{1}{2} - z)$ and $(-x, -\frac{1}{2} + y, \frac{1}{2} - z)$, respectively.

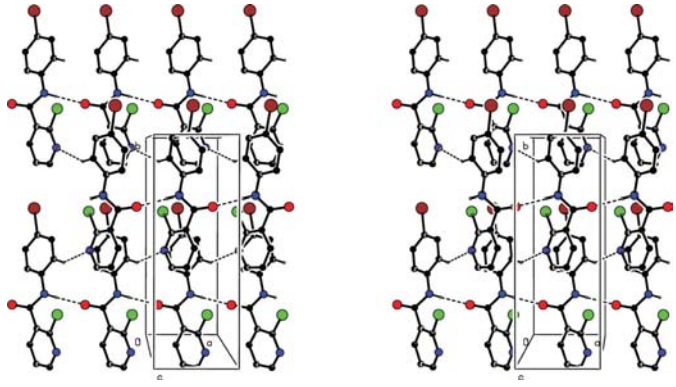

Figure 17
Stereoview of part of the crystal structure of (V) showing the formation of a hydrogen-bonded (001) sheet of $R_4^4(22)$ rings. For the sake of clarity, the H atoms not involved in the motifs shown have been omitted.

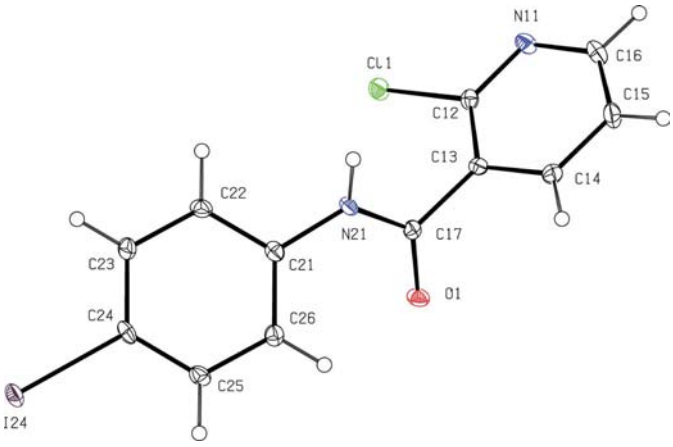

Figure 18
The molecule of (VI) showing the atom-labelling scheme. Displacement ellipsoids are drawn at the 30% probability level.

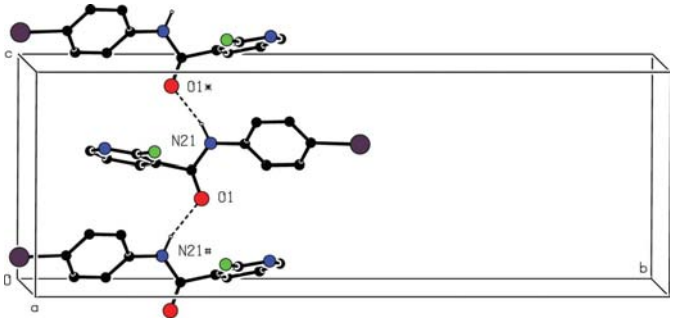

Figure 19
Part of the crystal structure of (VI) showing the formation of a hydrogen-bonded $C(4)$ chain along [001]. For the sake of clarity, the H atoms bonded to C atoms have been omitted. The atoms marked with an asterisk (*) or a hash (#) are at the symmetry positions $(x, \frac{1}{2}-y, \frac{1}{2}+z)$ and $(x, \frac{1}{2}-y, -\frac{1}{2}+z)$, respectively.

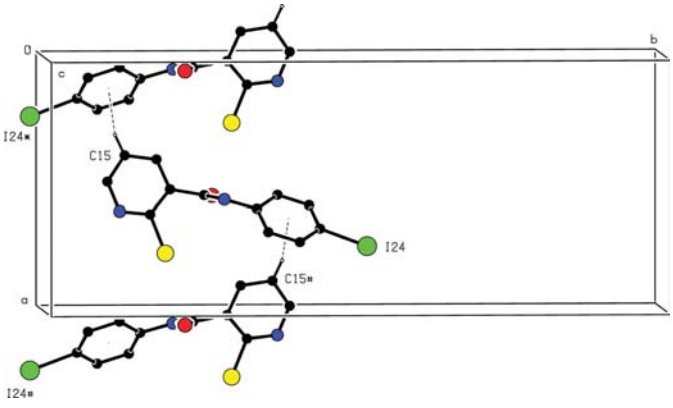

Figure 20
Part of the crystal structure of (VI) showing the formation of a hydrogen-bonded chain along [100]. For the sake of clarity, the H atoms not involved in the motif shown have been omitted. The atoms marked with an asterisk (*) or a hash (#) are at the symmetry positions $(-\frac{1}{2}+x, \frac{1}{2}-y, 1-z)$ and $(\frac{1}{2}+x, \frac{1}{2}-y, 1-z)$, respectively.

hydrogen bonds and aromatic $\pi\cdots\pi$ stacking interactions are both absent.

3.3.8. Compound (VIII). The structure of the 4-cyanophenyl compound (VIII) (Fig. 25) contains N—H···N, C—H···N and C—H···O hydrogen bonds (Table 3), as well as aromatic $\pi\cdots\pi$ stacking interactions; the resulting three-dimensional structure is of considerable complexity, although it is readily analysed in terms of its constituent one-dimensional sub-structures. Within the asymmetric unit, the amido N21 atom acts as a hydrogen-bond donor to the cyano N44 atom: similarly, the amido atom N41 at (x, y, z) acts as a donor to the cyano N24 atom at $(-2+x, 1+y, z)$, so generating by translation a $C_2^2(16)$ chain running parallel to the $[2\bar{1}0]$ direc-

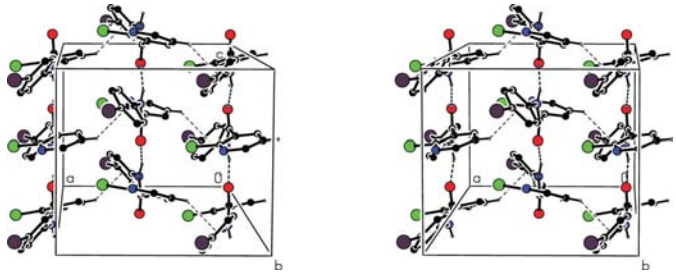

Figure 21
Stereoview of part of the crystal structure of (VI) showing the formation of a hydrogen-bonded (010) sheet. For the sake of clarity, the H atoms not involved in the motifs shown have been omitted.

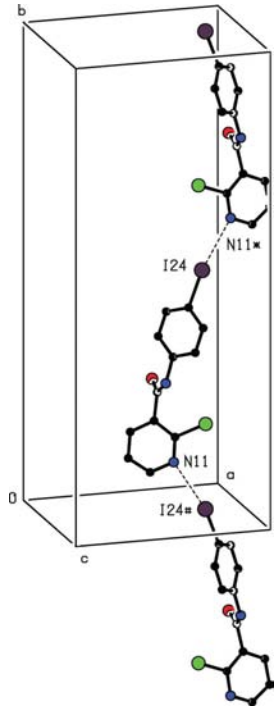

Figure 22
Part of the crystal structure of (VI) showing the formation of an iodo···N(pyridyl) chain along [010]. For the sake of clarity, the H atoms have been omitted. The atoms marked with an asterisk (*) or a hash (#) are at the symmetry positions $(\frac{3}{2}-x, \frac{1}{2}+y, z)$ and $(\frac{3}{2}-x, -\frac{1}{2}+y, z)$, respectively.

tion (Fig. 26). In contrast to the simple chain generated by the hard hydrogen bonds, the soft hydrogen bonds generate both molecular ladders and chains of rings (Bernstein *et al.*, 1995).

Atoms C15 and C35 in the bimolecular aggregate at (x, y, z) act as hydrogen-bond donors respectively to atoms O11 and O31 in the aggregate at $(-1+x, y, z)$. The individual C—H···O hydrogen bonds each generate by translation a $C(6)$ chain along [100] and, together with the N—H···N hydrogen bond within the bimolecular aggregate, they generate a chain of edge-fused $R_4^4(32)$ rings (Fig. 27). Alternatively, this motif can be regarded as a molecular ladder, in which the $C(6)$ chains form the uprights, and N—H···N hydrogen bonds form part of each rung.

In a similar way, the C25 and C45 atoms in the bimolecular aggregate at (x, y, z) act as hydrogen-bond donors respectively to pyridyl atoms N11 and N31 in the aggregate at $(1+x, -1+y, z)$. The individual C—H···N hydrogen bonds each generate by translation a $C(9)$ chain along $[1\bar{1}0]$ and together with the N—H···N hydrogen bond within the bimolecular aggregate they generate a chain of edge-fused $R_4^4(28)$ rings (Fig. 28). As before, this motif can be regarded as a molecular ladder, with the $C(9)$ chains now forming the uprights and with the N—H···N hydrogen bonds in the rungs.

Finally, atoms C14 and C34 at (x, y, z) acts as hydrogen-bond donors respectively to atoms O11 at $(1-x, -y, 1-z)$ and O31 at $(-1-x, 1-y, -z)$, so generating two distinct $R_2^2(10)$ rings, both centrosymmetric, and centred respectively

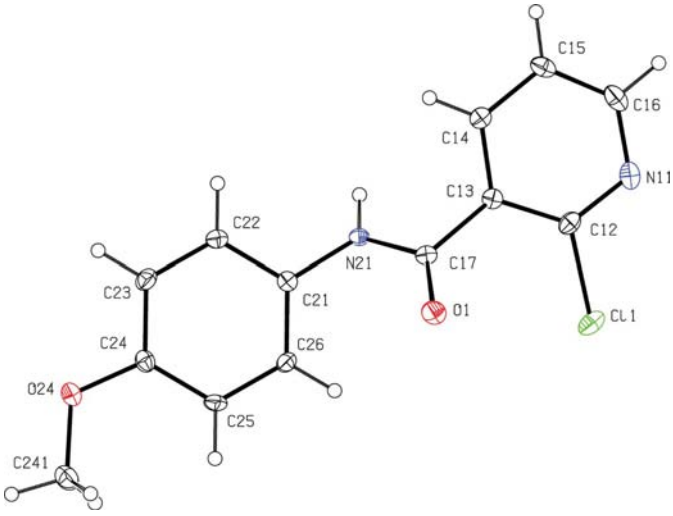

Figure 23
The molecule of (VII) showing the atom-labelling scheme. Displacement ellipsoids are drawn at the 30% probability level.

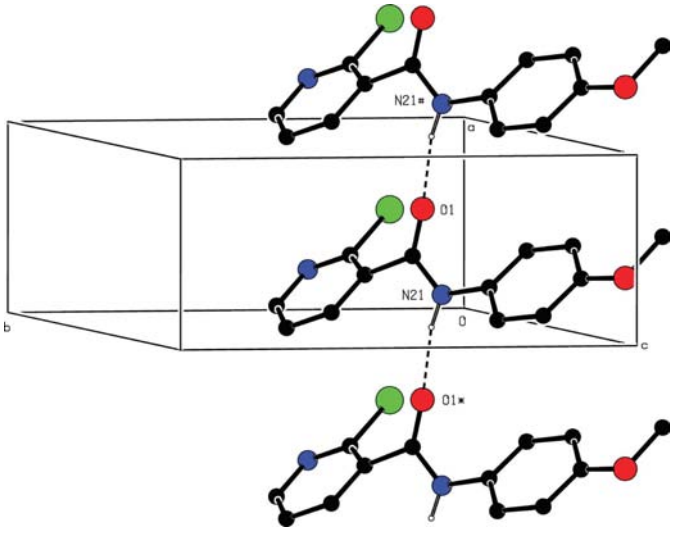

Figure 24
Part of the crystal structure of (VII) showing the formation of a hydrogen-bonded $C(4)$ chain along [100]. For the sake of clarity, the H atoms bonded to C atoms have been omitted. The atoms marked with an asterisk (*) or a hash (#) are at the symmetry positions $(-1+x, y, z)$ and $(1+x, y, z)$, respectively.

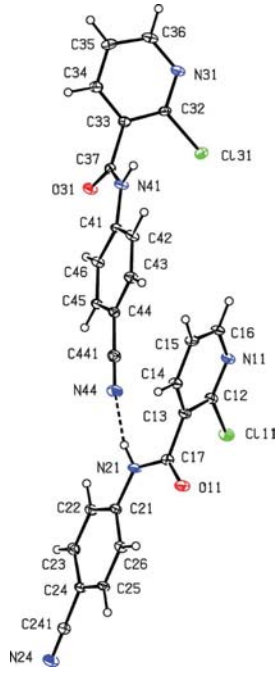

Figure 25
The two independent molecules of (VIII) showing the atom-labelling scheme and the N—H···N hydrogen bond within the asymmetric unit. Displacement ellipsoids are drawn at the 30% probability level.

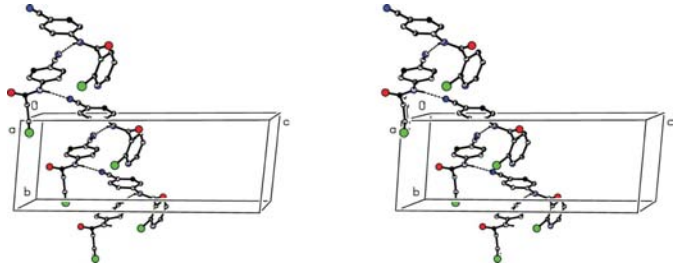

Figure 26
Stereoview of part of the crystal structure of (VIII) showing the formation of a $C_2^2(16)$ chain along $[2\bar{1}0]$ built from N—H···N hydrogen bonds. For the sake of clarity, the H atoms bonded to C atoms have been omitted.

at $(\frac{1}{2}, 0, \frac{1}{2})$ and $(-\frac{1}{2}, \frac{1}{2}, 0)$. The combination of these two rings, together with the N—H···N hydrogen bond within the asymmetric unit, then generates by inversion a chain of rings running parallel to the $[2\bar{1}1]$ direction (Fig. 29). This chain, in turn, is reinforced by a combination of two $\pi\cdots\pi$ stacking interactions. The pyridyl rings containing N11 in the molecules are (x, y, z) and $(1-x, 1-y, 1-z)$ and are parallel with an interplanar spacing of 3.426 (2) Å; the ring-centroid separation is 3.589 (2) Å, corresponding to a ring offset of 1.069 (2) Å; similarly, the pyridyl rings containing N31 in the molecules at (x, y, z) and $(-1-x, 2-y, -z)$ have an interplanar spacing of 3.334 (2) Å, with a ring-centroid separation of 3.658 (2) Å and ring offset of 1.505 (2) Å. These two interactions are centred across the inversion centres at $(\frac{1}{2}, \frac{1}{2}, \frac{1}{2})$ and $(-\frac{1}{2}, 1, 0)$, respectively, and their combination thus generates a second $[2\bar{1}1]$ substructure (Fig. 30). The combination of chains along [100], $[1\bar{1}0]$, $[2\bar{1}0]$ and $[2\bar{1}1]$ suffices to generate a continuous three-dimensional framework structure.

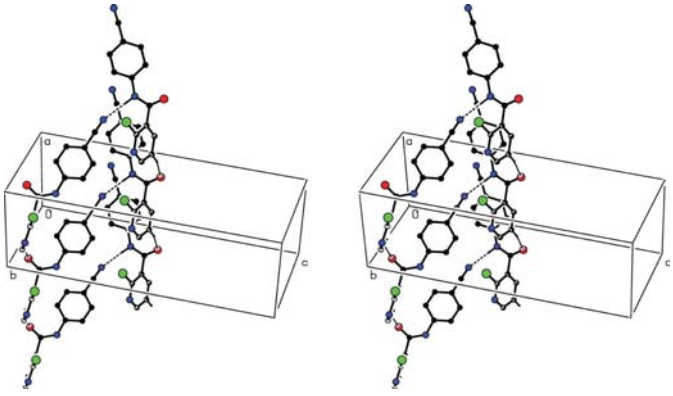

Figure 27
Stereoview of part of the crystal structure of (VIII) showing the formation of a chain of edge-fused $R_4^4(32)$ rings along [100] built from N—H···N and C—H···O hydrogen bonds. For the sake of clarity, the H atoms bonded to C atoms, but not involved in the motif shown, have been omitted.

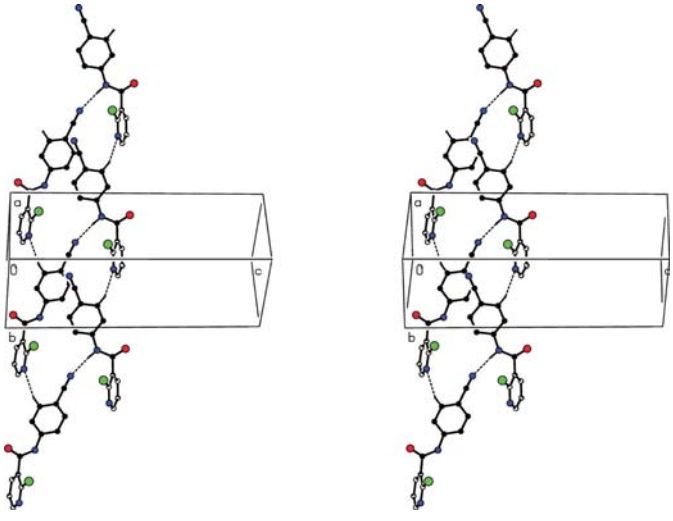

Figure 28
Stereoview of part of the crystal structure of (VIII) showing the formation of a chain of edge-fused $R_4^4(28)$ rings along $[1\bar{1}0]$ built from N—H···N and C—H···N hydrogen bonds. For the sake of clarity, the H atoms bonded to C atoms, but not involved in the motif shown, have been omitted.

3.3.9. Compound (IX). The structure of the 4-nitrophenyl analogue (IX) has recently been described (de Souza *et al.*, 2005) and here we briefly summarize its supramolecular behaviour. Compound (IX) crystallizes in the space group $P2_1/n$ with $Z' = 2$, and the molecules are linked by two independent N—H···N hydrogen bonds into $C_2^2(12)$ chains in which the two independent molecules alternate: however, the amidic N—H···O hydrogen bonds which characterize (II)–(VIII), although not (I), are absent from the structure of (IX).

3.3.10. General comments on the structures. Although the approximately isosteric requirements of methyl and chloro substituents on aryl rings often lead to the isomorphism of corresponding pairs of compounds, the unit-cell dimension and Z' values (Table 1) for (II) (X = CH_3) and (IV) (X = Cl) here are entirely distinct. Likewise, the four 4-halogenophenyl derivatives (III)–(VI) all crystallize in different space groups, one triclinic, two monoclinic and one orthorhombic. In contrast to this, we have recently observed:

(i) that the 4-substituted anilinium 2-carboxy-4-nitrobenzoates $[4\text{-}XC_6H_4NH_3]^+\cdot[C_8H_4NO_6]^-$, for X = H, Cl, Br and I, are all isomorphous and approximately isostructural (Glidewell *et al.*, 2005);

(ii) that a series of cyclopenta[*g*]pyrazolo[1,5-*a*]pyrimidines carrying 4-methylphenyl, 4-chlorophenyl or 4-bromophenyl substituents are all strictly isostructural (Portilla *et al.*, 2005); and

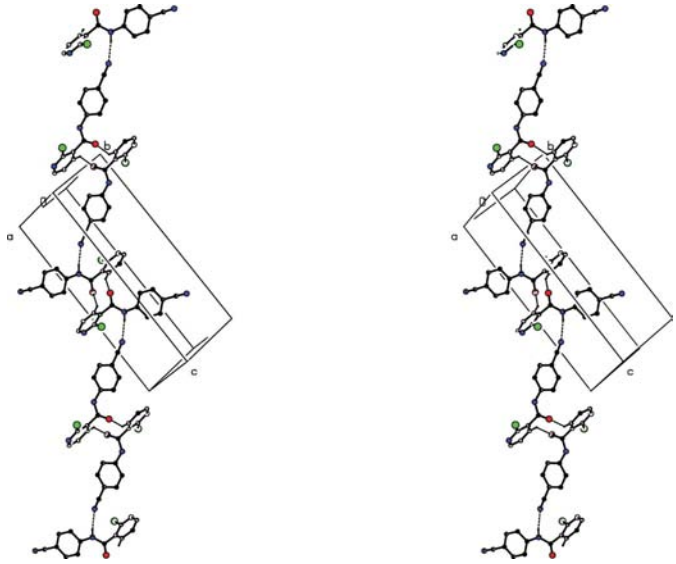

Figure 29
Stereoview of part of the crystal structure of (VIII) showing the formation of a chain of $R_2^2(10)$ rings along $[2\bar{1}1]$ built from N—H···N and C—H···O hydrogen bonds. For the sake of clarity, the H atoms bonded to C atoms, but not involved in the motif shown, have been omitted.

(iii) that a pair of benzo[*f*]pyrazolo[3,4-*b*]quinolines carrying 4-chlorophenyl or 4-bromophenyl substituents are also strictly isostructural (Serrano *et al.*, 2005*a*,*b*).

As the single substituent in the aryl ring is varied within the series (I)–(IX), so too are the direction-specific intermolecular interactions which are manifested in the supramolecular structures. A very common supramolecular motif found in the crystal structures of simple amides is the formation of simple $C(4)$ chains built from N—H···O hydrogen bonds, with corresponding $C_2^2(8)$ chains in some cases where $Z' = 2$. Such chains occur in (II), where the chain is of $C_2^2(8)$ type; in (IV), where there are four independent $C(4)$ chains, and in (V), (VI) and (VII), each of which forms a single $C(4)$ chain. It is striking how readily this motif can be disrupted when alternative hydrogen-bond acceptor sites are available, so that the amidic N—H donor has a pyridyl N acceptor in each of (I), (VIII) and (IX), while in (III) the water O atom acts as the acceptor to form the amidic N—H bond (Table 3). Despite the acceptor role for the pyridyl N atom manifested in (I), (VIII) and (IX), this potential acceptor is completely inactive in each of (II), (IV) and (VI), while in (III) and (V) this site acts as the acceptor in O—H···N and C—H···N hydrogen bonds, respectively. No obvious pattern of behaviour can be discerned here and any attempt to rationalize such behaviour would necessarily be largely, if not entirely, speculative: in this connection, it should perhaps be emphasized that the intermolecular forces involved here are all fairly weak and soft, and not readily susceptible to quantitative modelling.

For (IV), where X = Cl, (VII) where X = OMe and (IX) where X = NO_2 (de Souza *et al.*, 2005), the supramolecular structures are all one-dimensional, with isolated chains built from N—H···O hydrogen bonds in (VII), similar chains linked in pairs by C—H···π(arene) hydrogen bonds in (IV), and chains built from N—H···N hydrogen bonds in (IX). Compounds (IV) and (IX) differ further in that (IV), where $Z' = 4$, contains four independent chains, each containing a single molecular type, whereas (IX), where $Z' = 2$, contains a single chain where the two independent molecules alternate.

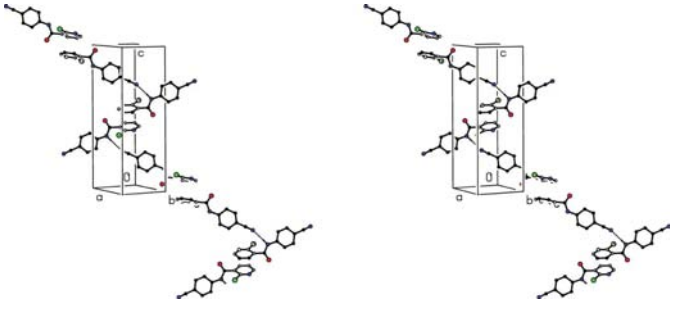

Figure 30
Stereoview of part of the crystal structure of (VIII) showing the formation of a π-stacked chain along [2$\bar{1}$1]. For the sake of clarity, the H atoms have been omitted.

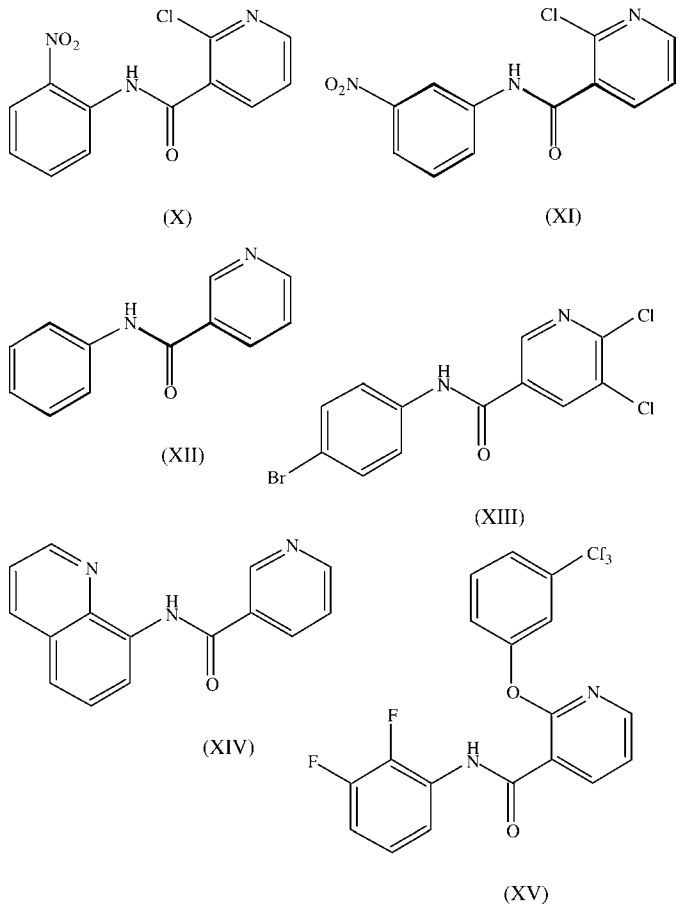

The structures of compounds (I), where X = H, (II), where X = Me, (III), where X = F, and (V), where X = Br, are all two-dimensional. N—H···N hydrogen bonds are present only in the structure of (I); C—H···O and C—H···π(arene) hydrogen bonds are present only in the structure of (II); O—H···O and O—H···N hydrogen bonds, and aromatic π···π stacking interactions are present only in the structure of (III); and C—H···N hydrogen bonds are present only in the structure of (V). For the two compounds with three-dimensional supramolecular structures, there are no direction-specific intermolecular interactions in common: the structure of (VI), where X = I, is built from N—H···O and C—H···π(arene) hydrogen bonds, and iodo···pyridyl interactions, while the structure of (VIII), where X = CN, is built from N—H···N, C—H···N and C—H···O hydrogen bonds.

3.3.11. Compounds closely related to (I)–(IX). Here we briefly comment on the supramolecular structures of some closely related compounds, including two isomers (X) and (XI) of (IX) (de Souza *et al.*, 2005), and (XII)–(XV) retrieved from the Cambridge Structural Database (CSD; Allen, 2002).

In (X), the only N—H···O hydrogen bond is intramolecular, so that again the formation of a $C(4)$ chain has readily been prevented: the molecules of (X) are linked into chains of centrosymmetric edge-fused $R_2^2(14)$ and $R_4^4(24)$ rings by two independent C—H···.O hydrogen bonds, while the pyridyl N atom is inactive as an acceptor. In the isomeric compound

(XI), which unexpectedly crystallizes as a stoichiometric monohydrate just like compound (III), the amidic N—H bond acts as a hydrogen-bond donor to the water molecule, and these bimolecular aggregates are linked by a combination of O—H···N and O—H···O hydrogen bonds to form a chain of edge-fused rings containing two different types of $R_4^4(16)$ ring. Thus, despite the different composition and constitutions of (III) and (XI), their supramolecular aggregation patterns show a considerable degree of similarity.

The unsubstituted amide (XII) (CSD code PYDCXA10; Gdaniec *et al.*, 1979), which may be regarded as the parent compound for this whole series, forms simple C(4) chains built from N—H···O hydrogen bonds, and these chains are linked in pairs by a centrosymmetric $\pi\cdots\pi$ stacking interaction. In the dichloro compound (XIII) (CSD code HIFWUO; Jethmalani *et al.*, 1996), a combination of N—H···N and C—H···N hydrogen bonds generates a $C(3)C(6)[R_2^1(7)]$ chain of rings, but no N—H···O hydrogen bonds are present.

The ease with which the $C(4)$ motif can be disrupted, not only by the presence of water molecules in the structure, but also by intramolecular hydrogen bonds, is shown both by (X), and by (XIV) (CSD code MURWUR; Zhang *et al.*, 2002) and (XV) (CSD code ZIKWEX; Pèpe *et al.*, 1995), where the amidic N—H bonds participate respectively in intramolecular N—H···N and N—H···O hydrogen bonds. The supramolecular structure of (XIV) consists of simple $C(6)$ chains built from C—H···O hydrogen bonds, while the structure of (XV) consists of effectively isolated molecules with no direction-specific intermolecular interactions of any kind.

4. Concluding remarks

The variations in the unit-cell dimensions in (I)–(IX) and the consequent absence of any isomorphisms, together with the very wide variations in the active intermolecular interactions and in the resulting supramolecular structures, both for these compounds and for the related compounds (X)–(XV), raise the question of whether supramolecular structures of this type, dependent on weak intermolecular forces, are likely to become reliably predictable in the foreseeable future.

We thank the EPSRC National Crystallography Service, University of Southampton, UK, for collecting the X-ray data for (I) and (III)–(VIII). Data for (II) were collected on Daresbury SRS Station 9.8, for which we thank the EPSRC-funded synchrotron crystallography service and Professor W. Clegg. JLW and SMSVW thank CNPq and FAPERJ for financial support.

References

Allen, F. H. (2002). *Acta Cryst.* B**58**, 380–388.
Bernstein, J., Davis, R. E., Shimoni, L. & Chang, N.-L. (1995). *Angew. Chem. Int. Ed. Engl.* **34**, 1555–1573.
Bruker (2004). *APEX*2, *SADABS* and *SAINT*, Version 6.02*a*. Bruker AXS Inc., Madison, Wisconsin, USA.
Cernik, R. J., Clegg, W., Catlow, C. R. A., Bushnell-Wye, G., Flaherty, J. V., Greaves, G. N., Hamichi, M., Burrows, I., Taylor, D. J. & Teat, S. J. (1997). *J. Synchrotron Rad.* **4**, 279–286.
Ferguson, G. (1999). *PRPKAPPA*. University of Guelph, Canada.
Flack, H. D. (1983). *Acta Cryst.* A**39**, 876–881.
Gdaniec, M., Jaskolski, M. & Kosturkiewicz, Z. (1979). *Pol. J. Chem.* **53**, 2563–2569.
Glidewell, C., Low, J. N., Skakle, J. M. S. & Wardell, J. L. (2005). *Acta Cryst.* C**61**, o276–o280.
Hooft, R. W. W. (1999). *Collect.* Nonius BV, Delft, The Netherlands.
Jethmalani, J. M., Camp, A. G., Soman, N. G., Hawley, J. W., Setliff, F. L. & Holt, E. M. (1996). *Acta Cryst.* C**52**, 438–441.
McArdle, P. (2003). *OSCAIL* for Windows, Version 10. Crystallography Centre, Chemistry Department, NUI Galway, Ireland.
Otwinowski, Z. & Minor, W. (1997). *Methods in Enzymology*, Vol. 276, *Macromolecular Crystallography*, Part A, edited by C. W. Carter Jr & R. M. Sweet, pp. 307–326. New York: Academic Press.
Pèpe, G., Pfefer, G. & Boistelle, R. (1995). *Acta Cryst.* C**51**, 2671–2672.
Portilla, J., Quiroga, J., Cobo, J., Low, J. N. & Glidewell, C. (2005). *Acta Cryst.* C**61**, o452–o456.
Serrano, H., Quiroga, J., Cobo, J., Low, J. N. & Glidewell, C. (2005*a*). *Acta Cryst.* E**61**, o1058–o1060.
Serrano, H., Quiroga, J., Cobo, J., Low, J. N. & Glidewell, C. (2005*b*). *Acta Cryst.* E**61**, o1702–o1703.
Sheldrick, G. M. (1997*a*). *SHELXS*97 University of Göttingen, Germany.
Sheldrick, G. M. (1997*b*). *SHELXL*97. University of Göttingen, Germany.
Sheldrick, G. M. (2003). *SADABS*, Version 2.10. University of Göttingen, Germany.
Souza, M. V. N. de, Vasconcelos, T. R. A., Wardell, S. M. S. V., Wardell, J. L., Low, J. N. & Glidewell, C. (2005). *Acta Cryst.* C**61**, o204–o208.
Spek, A. L. (2003). *J. Appl. Cryst.* **36**, 7–13.
Starbuck, J., Norman, N. C. & Orpen, A. G. (1999). *New J. Chem.* **23**, 969–972.
Wilson, A. J. C. (1976). *Acta Cryst.* A**32**, 994–996.
Zhang, J.-Y., Tu, C., Lin, J., Fun, H.-K., Chantrapromma, S., You, X.-Z. & Guo, Z.-J. (2002). *Chin. J. Inorg. Chem.* **18**, 554–558.